JACS
JOURNAL OF THE AMERICAN CHEMICAL SOCIETY
Article
pubs.acs.org/JACS

Incorporation of Pendant Bases into Rh(diphosphine)$_2$ Complexes: Synthesis, Thermodynamic Studies, And Catalytic CO_2 Hydrogenation Activity of $[Rh(P_2N_2)_2]^+$ Complexes

Alyssia M. Lilio,[†] Mark H. Reineke,[†] Curtis E. Moore,[†] Arnold L. Rheingold,[†] Michael K. Takase,[‡] and Clifford P. Kubiak*,[†]

[†]Department of Chemistry and Biochemistry, University of California, San Diego, 9500 Gilman Drive, La Jolla, California 92093-0358, United States

[‡]Beckman Institute, California Institute of Technology, 1200 East California Blvd., Pasadena, California 91125, United States

Supporting Information

ABSTRACT: A series of five $[Rh(P_2N_2)_2]^+$ complexes (P_2N_2 = 1,5-diaza-3,7-diphosphacyclooctane) have been synthesized and characterized: $[Rh(P^{Ph}{}_2N^{Ph}{}_2)_2]^+$ (**1**), $[Rh(P^{Ph}{}_2N^{Bn}{}_2)_2]^+$ (**2**), $[Rh(P^{Ph}{}_2N^{PhOMe}{}_2)_2]^+$ (**3**), $[Rh(P^{Cy}{}_2N^{Ph}{}_2)_2]^+$ (**4**), and $[Rh(P^{Cy}{}_2N^{PhOMe}{}_2)_2]^+$ (**5**). Complexes **1**−**5** have been structurally characterized as square planar rhodium bis-diphosphine complexes with slight tetrahedral distortions. The corresponding hydride complexes **6**−**10** have also been synthesized and characterized, and X-ray diffraction studies of $HRh(P^{Ph}{}_2N^{Bn}{}_2)_2$ (**7**), $HRh(P^{Ph}{}_2N^{PhOMe}{}_2)_2$ (**8**) and $HRh(P^{Cy}{}_2N^{Ph}{}_2)_2$ (**9**) show that the hydrides have distorted trigonal bipyramidal geometries. Equilibration of complexes **2**−**5** with H_2 in the presence of 2,8,9-triisopropyl-2,5,8,9-tetraaza-1-phosphabicyclo[3,3,3]-undecane (Verkade's base) enabled the determination of the hydricities and estimated pK_a's of the Rh(I) hydride complexes using the appropriate thermodynamic cycles. Complexes **1**−**5** were active for CO_2 hydrogenation under mild conditions, and their relative rates were compared to that of $[Rh(depe)_2]^+$, a nonpendant-amine-containing complex with a similar hydricity to the $[Rh(P_2N_2)_2]^+$ complexes. It was determined that the added steric bulk of the amine groups on the P_2N_2 ligands hinders catalysis and that $[Rh(depe)_2]^+$ was the most active catalyst for hydrogenation of CO_2 to formate.

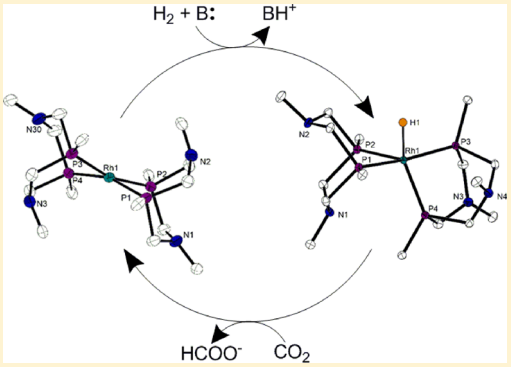

INTRODUCTION

The incorporation of functional groups into the second coordination sphere of molecular catalysts has been extensively studied as a strategy to produce simple functional mimics of nature's most active catalysts.[1] Metal complexes with cyclic diphosphine P_2N_2 (1,5-diaza-3,7-diphosphacyclooctane) ligands[2] are a prominent example of this approach, with the pendant nitrogen base arms of the P_2N_2 ligand helping to shuttle protons to and from the metal center. In $Ni(P_2N_2)_2$ complexes, this proton shuttling activity enables some of the highest turnover frequencies for proton reduction/H_2 oxidation known by an artificial catalyst,[3] as well as diverse small-molecule reactivity including oxygen reduction[4] and formate oxidation electrocatalysis.[5] In most cases, these catalytic mechanisms involve transient Ni−H species and protonated pendant bases.[6]

We became interested in the use of $M(P_2N_2)_2$ complexes for CO_2 reduction because of their potential to deliver both a proton and a hydride to CO_2, producing formic acid. We initially studied $Ni(P_2N_2)_2$ complexes for this purpose, but quickly found that they thermodynamically favor the reverse reaction, the oxidative decomposition of formic acid to CO_2 and H_2.[5] Given its rich hydrogenation chemistry,[7] Rh(I) was a natural choice to make $M(P_2N_2)_2$ complexes that would favor hydride transfer to CO_2, allowing us to study the influence of the second coordination sphere on CO_2 hydrogenation. Rhodium complexes have been used for the hydrogenation of a variety of substrates, including alkenes,[8] nitriles,[9] and N-heterocycles.[10] A number of rhodium bis-diphosphine complexes are also suitable for carbon dioxide hydrogenation.[11] Tuning of the second coordination sphere of rhodium bis-diphosphine catalysts could potentially lead to rate enhancements, as has been observed in other CO_2 hydrogenation catalysts.[12] Recently, pendant bases have been incorporated into this type of catalyst through PNP diphosphine ligands, which contain amines in the second coordination sphere and mono- and dipeptides in the outer coordination sphere, and it was found that the addition of an amine in the second coordination sphere increased catalytic rates for CO_2 hydrogenation by increasing the electron density of the metal center, but electron-withdrawing substituents in the outer coordination sphere decreased activity.[13] However, no true Rh analogue to

Received: April 24, 2015
Published: June 4, 2015

DOI: 10.1021/jacs.5b04291
J. Am. Chem. Soc. 2015, 137, 8251−8260

the well-studied $Ni(P_2N_2)_2$ system has been presented in the literature.

We set out to synthesize rhodium diphosphine complexes with P_2N_2 ligands to extend the chemistry of the P_2N_2 platform to rhodium, map out thermodynamic properties of these complexes relevant to catalysis, and to explore the effects of the pendant-base-containing ligands on the hydrogenation of CO_2. Herein we report the synthesis and characterization of these complexes and the corresponding rhodium hydrides, as well as thermodynamic measurements of K_{eq} for oxidative H_2 addition, and hydricities (hydride donor abilities) and acidities of the monohydride species. We also report the CO_2 hydrogenation activity of these complexes and discuss how substituent effects may be changing the rates for CO_2 hydrogenation.

RESULTS AND DISCUSSION

Synthesis of and Characterization of $[Rh(P_2N_2)_2]BF_4$ Complexes. A series of P_2N_2 ligands was chosen in order to systematically vary the hydricities of the rhodium compounds and the basicities of the pendant amines (Figure 1). The ligands

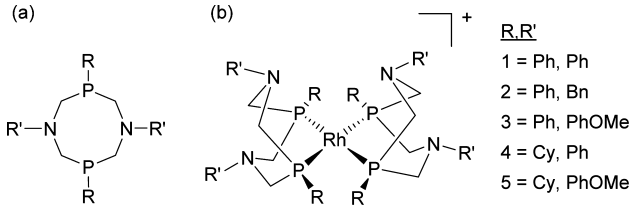

Figure 1. Structure of a P_2N_2 ligand (**a**) and a $[Rh(P_2N_2)_2]^+$ complex (**b**).

$P^{Cy}_2N^{Ph}_2$, $P^{Ph}_2N^{Ph}_2$, $P^{Ph}_2N^{Bn}_2$, $P^{Ph}_2N^{PhOMe}_2$, and $P^{Cy}_2N^{PhOMe}_2$ were synthesized as previously reported.[5a,14] Procedures for the synthesis of Rh(I) complexes **1**−**5** were adapted from previously reported methods.[15] Stoichiometric amounts of rhodium(I) chloride 1,5-cyclooctadiene dimer and $AgBF_4$ were dissolved in acetone, the precipitated AgCl was filtered out, and the filtrate was added to a methylene chloride solution containing 2 equiv of ligand per Rh center and allowed to react overnight. The solvent was reduced in volume, and the product was precipitated with the addition of diethyl ether to yield complexes **1**−**5**, isolated as yellow powders. All complexes were characterized by elemental analysis, mass spectroscopy, and ^1H and $^{31}P\{^1H\}$ NMR spectroscopy. The ^{31}P NMR of each shows a characteristic doublet in the range of −3 to 10 ppm with a $^1J_{P-Rh}$ coupling constant of 121−124 Hz. The ^{31}P shifts and coupling constants are consistent with a chelating phosphine bound to Rh(I).[15,16] The single sharp ^{31}P resonance is indicative of all four phosphorus atoms being magnetically equivalent.

Solid-state structures of complexes **1**−**5** were obtained via single-crystal diffraction (Figure 2) and selected bond lengths and angles are shown in Table 1. Complex **1** was isolated as the PF_6 salt since it crystallized more easily than the BF_4 salt. The two salts are indistinguishable by NMR and mass spectroscopy. Suitable crystals for X-ray diffraction of all complexes were grown from the vapor diffusion of diethyl ether into saturated acetonitrile solutions. Complexes **1**−**5** show very similar structures in which both P_2N_2 ligands are coordinated to the Rh through the phosphorus atoms, with nominally square planar geometries around the Rh(I) centers. The small deviations from square planar geometry can be best compared via their dihedral angles, which are listed in Table 1. In **1**−**4**, the ligands consistently crystallize in alternating chair−boat−chair−boat conformations with respect to the two six-membered metallocycles formed by each ligand clockwise around the central Rh atom. The complexes also have very similar dihedral angles, ranging from 23−26°. In complex **5**, both ligands crystallize in boat−boat conformations. The geometry of complex **5** is more distorted toward tetrahedral, with a dihedral angle of 32.3°. In all complexes, the ligands show similar bite angles (79−82°). The measured bite angles are smaller by an average of 1° when compared to the analogous Ni complexes and 0.6° smaller when compared to the Pd complexes. The Rh−P bond lengths of the five structures are on the order of 2.28 Å, which is slightly longer (0.08 Å) when compared to the analogous Ni complexes, but slightly shorter (0.05 Å) when compared to the Pd complexes.

Synthesis of $HRh(P_2N_2)_2$ Complexes. $HRh(P_2N_2)_2$ complexes **6**−**10** were synthesized by reacting the $[Rh(P_2N_2)_2]BF_4$ complexes with 1.2 equiv of $NaHBEt_3$ in toluene. The solutions were stirred overnight and then filtered to remove any precipitated $NaBF_4$. The filtrates were evaporated and the residues were dissolved in a minimum of THF and layered with pentane to induce precipitation of the products, which were isolated as yellow to red-orange powders and were characterized by elemental analysis, mass spectroscopy, and ^1H and $^{31}P\{^1H\}$ NMR spectroscopy. In the ^1H NMR spectra, the hydride resonances appear as a doublet of quintets, consistent with splitting by one Rh and four equivalent phosphorus atoms. The $^{31}P\{^1H\}$ spectra contain one resonance that appears as a doublet ($^1J_{P-Rh}$ = 128−132 Hz) downfield by about 10 ppm as compared to the parent diphosphine complex.

Crystals of the neutral rhodium hydrides **7**−**9** suitable for X-ray diffraction were obtained by vapor diffusion of pentane into saturated THF solutions (Figure 3). Selected bond lengths and angles are given in Table 2. The hydride ligands of these complexes were located in the difference map. The geometries of the neutral hydrides can be described as distorted trigonal bipyramidal with one phosphorus atom (P4) and the hydride ligand occupying the axial positions. Complexes of the $[HM(diphosphine)_2]^{n+}$ type (M = Co, Pd, Pt) have been shown to adopt this geometry over a square pyramidal geometry.[17] Deviation from trigonal bipyramidal geometry is apparent in the H−Rh−P4 bond angles, which are significantly smaller than the expected 180° due to constraints imposed by the chelating ligands. The angles between the hydride ligands and the equatorial phosphorus atoms are also considerably less than the expected 90°. This bending of *cis* ligands toward hydrogen can be attributed to both steric and electronic effects.[17b,18] The Rh−H bond distances of 1.587(15) Å to 1.64(7) Å are in the range expected for Rh(I)−H bonds.[19] The Rh−P bond distances are slightly longer compared to those of the starting complexes.

In complex **7**, both P_2N_2 ligands crystallized in chair−boat conformations with the amine arm *cis* to the hydride ligand pointing away from the metal center. Two similar molecules crystallize in the asymmetric unit of complex **8**, and in both molecules, the equatorial P_2N_2 ligands take on chair−boat conformations with the amine in the boat conformation pointing toward the hydride ligand (average nonbonding N−H distance is 2.679 Å). The other P_2N_2 ligands take on the boat−boat conformation. In complex **9**, both P_2N_2 ligands take on chair−boat conformations. Similar to complex **8**, one of the amine arms of the P_2N_2 ligand is poised to interact with the

DOI: 10.1021/jacs.5b04291
J. Am. Chem. Soc. 2015, 137, 8251−8260

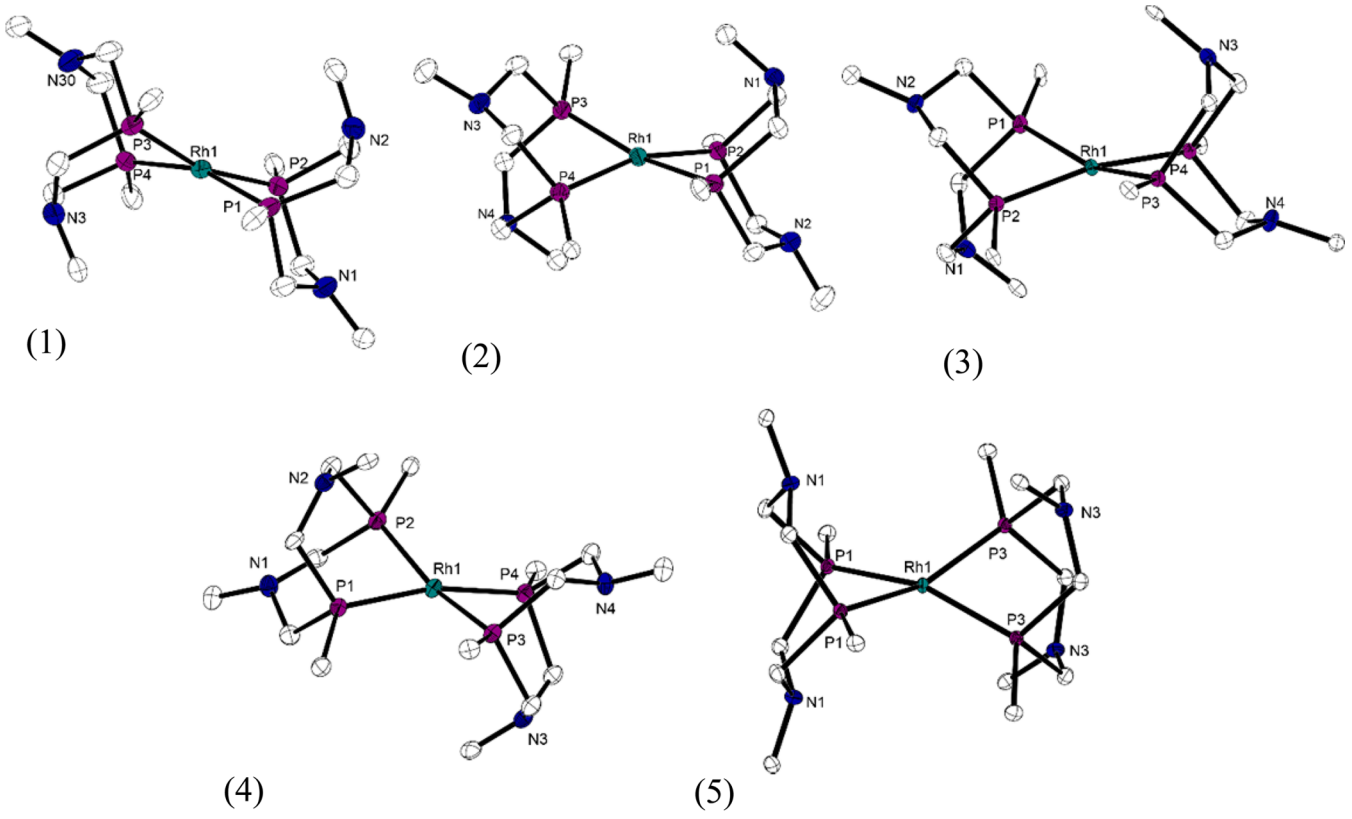

Figure 2. Thermal ellipsoid plots of the crystal structures of (**1**) $[Rh(P^{Ph}{}_2N^{Ph}{}_2)_2]^+$, (**2**) $[Rh(P^{Ph}{}_2N^{Bn}{}_2)_2]^+$, (**3**) $[Rh(P^{Ph}{}_2N^{PhOMe}{}_2)_2]^+$, (**4**) $[Rh(P^{Cy}{}_2N^{Ph}{}_2)_2]^+$, and (**5**) $[Rh(P^{Cy}{}_2N^{PhOMe}{}_2)_2]^+$, shown at the 50% probability level. For clarity, hydrogen atoms, uncoordinated counterions, and solvent molecules have been omitted, and only the first carbon of the nitrogen and phosphorus substituents are shown.

Table 1. Selected Bond Lengths [Å], Bond Angles [°], and Dihedral Angles [°] of $[Rh(P_2N_2)_2]^+$ Complexes[a]

(**1**) $Rh(P^{Ph}{}_2N^{Ph}{}_2)_2PF_6$		(**2**) $Rh(P^{Ph}{}_2N^{Bn}{}_2)_2BF_4$ a		$Rh(P^{Ph}{}_2N^{Bn}{}_2)_2BF_4$ b	
Rh1−P1	2.2863(7)	Rh1−P1	2.2877(10)	Rh1−P1′	2.2871(10)
Rh1−P2	2.2663(7)	Rh1−P2	2.2724(9)	Rh1′−P2′	2.2718(9)
Rh1−P3	2.2706(7)	Rh1−P3	2.2669(10)	Rh1′−P3′	2.2658(9)
Rh1−P4	2.2715(7)	Rh1−P4	2.2819(9)	Rh1′−P4′	2.2793(9)
P2−Rh1−P1	81.03(2)	P1−Rh1−P2	80.02(3)	P1′−Rh1′−P2′	79.43(3)
P3−Rh1−P4	81.97(3)	P3−Rh1−P4	80.79(3)	P3′−Rh1′−P4′	79.96(3)
P1−Rh1−P4	162.17(3)	P1−Rh1−P3	165.57(4)	P3′−Rh1′−P1′	166.44(4)
P2−Rh1−P3	164.15(3)	P2−Rh1−P4	162.89(4)	P2′−Rh1′−P4′	163.16(4)
Dihedral	25.73	Dihedral	23.86	Dihedral	23.44
(**3**) $Rh(P^{Ph}{}_2N^{PhOMe}{}_2)_2BF_4$		(**4**) $Rh(P^{Cy}{}_2N^{Ph}{}_2)_2BF_4$		(**5**) $Rh(P^{Cy}{}_2N^{PhOMe}{}_2)_2BF_4$	
Rh1−P1	2.2954(9)	Rh1−P1	2.29208(9)	Rh1−P1#	2.2781(4)
Rh1−P2	2.2787(9)	Rh1−P2	2.2931(11)	Rh1−P1	2.2782(4)
Rh1−P3	2.27879(8)	Rh1−P3	2.2927(11)	Rh1−P3#	2.2829(4)
Rh1−P4	2.2879(8)	Rh1−P4	2.3166(10)	Rh1−P3	2.2828(4)
P1−Rh1−P2	81.68(3)	P1−Rh1−P2	80.70(4)	P1#−Rh1−P1	79.81(2)
P3−Rh1−P4	82.01(3)	P3−Rh1−P4	80.69(4)	P3#−Rh1−P3	79.30(2)
P1−Rh1−P3	161.97(3)	P1−Rh1−P4	164.71(4)	P1−Rh1−P3	159.494(15)
P2−Rh1−P4	169.03(3)	P2−Rh1−P4	164.83(4)	P1#−Rh1−P3#	159.493(15)
Dihedral	22.61	Dihedral	23.49	Dihedral	32.28

[a]For complex **2**, two molecules crystallize in the unit cell, and the bond lengths and bond angles of both are given as complex a and b.

hydride ligand (nonbonding N−H distance is 2.428 Å). Only one other $[HM(P_2N_2)_2]^{n+}$ structure, $[HNi(P^{iPr}{}_2N^{Ph}{}_2)_2]^+$, has been previously reported, although the hydride ligand could not be resolved in this case. In this structure, one arm of the P_2N_2 ligands is also pointed toward the expected location of the hydride ligand as it is in complexes **8** and **9**, indicating a possible hydrogen bonding interaction between the pendant amine and hydride ligand.[20] In the case of the nickel complexes, this interaction has also been observed in spectroscopic and computational data.[21] It should be noted that the interaction between the amine arm and the hydride ligand in the crystal structures of complexes **8** and **9** does not necessarily indicate an interaction in solution.

DOI: 10.1021/jacs.5b04291
J. Am. Chem. Soc. 2015, 137, 8251−8260

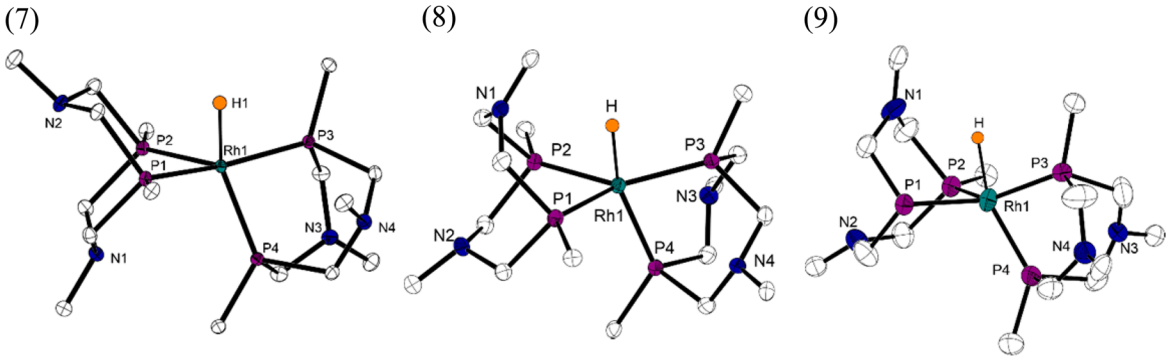

Figure 3. Thermal ellipsoid plots of the crystal structures of (**7**) $HRh(P^{Ph}{}_2N^{Bn}{}_2)_2$, (**8**) $HRh(P^{Ph}{}_2N^{PhOMe}{}_2)_2$, and (**9**) $HRh(P^{Cy}{}_2N^{Ph}{}_2)_2$ shown at the 50% probability level. For clarity, nonhydride hydrogen atoms and solvent molecules have been omitted, and only the first carbon of the nitrogen and phosphorus substituents are shown.

Table 2. Selected Bond Lengths [Å] and Bond Angles [°] of $HRh(P_2N_2)_2$ Complexes[a]

(**7**) $HRh(P^{Ph}{}_2N^{Bn}{}_2)_2$		(**8**) $HRh(P^{Ph}{}_2N^{PhOMe}{}_2)_2$ a		$HRh(P^{Ph}{}_2N^{PhOMe}{}_2)_2$ b	
Rh1−H1	1.587(15)	Rh1−H1	1.59(3)	Rh(1′)−HA	1.61(3)
Rh1−P1	2.2538(3)	Rh1−P1	2.2839(9)	Rh(1′)−P(1′)	2.2812(9)
Rh1−P2	2.3186(3)	Rh1−P2	2.2879(9)	Rh(1′)−P(2′)	2.3024(9)
Rh1−P3	2.2246(3)	Rh1−P3	2.2420(9)	Rh(1′)−P(3′)	2.2389(9)
Rh1−P4	2.2803(3)	Rh1−P4	2.2841(9)	Rh(1′)−P(4′)	2.2779(9)
H1−Rh1−P1	80.0(5)	H1−Rh1−P1	82(2)	P(1′)−Rh(1′)−HA	82.4(19)
H1−Rh−P2	95.5(5)	H1−Rh−P2	87(2)	P(2′)−Rh(1′)−HA	84.5(19)
H1−Rh1−P3	87.3(5)	H1−Rh1−P3	85(2)	P(3′)−Rh(1′)−HA	88.0(19)
H1−Rh1−P4	154.4(5)	H1−Rh1−P4	162(2)	P(4′)−Rh(1′)−HA	166(2)
P1−Rh1−P2	80.811(10)	P1−Rh1−P2	82.89(3)	P(1′)−Rh(1′)−P(2′)	82.07(3)
P3−Rh1−P4	81.254(11)	P3−Rh1−P4	78.94(3)	P(3′)−Rh(1′)−P(4′)	78.34(3)
(**9**) $HRh(P^{Cy}{}_2N^{Ph}{}_2)_2$					
Rh1−H1	1.64(7)	Rh1−P4	83(2)	P1−Rh1−P2	81.72(5)
Rh1−P1	2.2621(13)	H −Rh1−P1	79(2)	P3−Rh1−P4	79.32(5)
Rh1−P2	2.2598(14)	H −Rh1−P2	79(2)		
Rh1−P3	2.1967(14)	H −Rh1−P2	158(2)		

[a]For complex **8**, two molecules crystallize in the unit cell, and the bond lengths and bond angles of both are given as complex a and b.

Electrochemical Studies of $[Rh(P_2N_2)_2]BF_4$ Complexes. The cyclic voltammograms (CVs) of complexes **1**−**5** show single reversible 2-electron reductions (Figure 3) corresponding to the d^8/d^{10} couple, which are consistent with the electrochemistry of previously reported Rh(I) bis-diphosphine complexes.[15,22] The observed reductions are diffusion controlled, as indicated by linear plots of the peak current against the square root of the scan rate. The 2-electron nature of this couple is evident in the splitting of the cathodic and anodic peaks, which fall between the 60 mV expected for a completely reversible one-electron reduction and the 30 mV expected for a completely reversible 2-electron reduction (Table 3).[23] For comparison, the splitting of the II/I peaks for cobaltocene in the same set of experiments was 61 mV. Upon reduction, Rh(I) is expected to go from square planar to tetrahedral geometry based on structures of other d^8 and d^{10} complexes.[24] The reversibility of the electrochemical reduction suggests that the complexes are able to rapidly adjust their geometries on the electrochemical time scale. The ratios of the cathodic and anodic peak currents deviate somewhat from that expected for a fully reversible process, likely due to irreversible chemical processes which occur after reduction. CVs of each complex and plots of the peak current vs the square root of the scan rate can be found in the Supporting Information. Reduction potentials and peak splittings are given in Table 3.

Table 3. Reduction Potentials and CV Peak Data for the Series of $[Rh(P_2N_2)_2]BF_4$ Complexes[a]

	complex	$E_{1/2}(Rh^{I/-I})$ (V vs $FeCp_2^{+/0}$)	ΔE_p	i_{pc}/i_{pa}
1	$[Rh(P^{Ph}{}_2N^{Ph}{}_2)_2]^+$	−2.21	50	1.1
2	$[Rh(P^{Ph}{}_2N^{Bn}{}_2)_2]^+$	−2.43	48	1.3
3	$[Rh(P^{Ph}{}_2N^{PhOMe}{}_2)_2]^+$	−2.27	42	1.2
4	$[Rh(P^{Cy}{}_2N^{Ph}{}_2)_2]^+$	−2.39	50	1.4
5	$[Rh(P^{Cy}{}_2N^{PhOMe}{}_2)_2]^+$	−2.45	42	1.6

[a]Conditions: 1 mM complex in 0.2 M NBu_4PF_6 in acetonitrile solution, 100 mV/s scan rate, 3 mm glassy carbon working electrode.

The reduction potentials of complexes **1**−**5** generally follow the trend that complexes with more donating cyclohexyl substituents on the phosphine have reduction potentials ~0.2 V more negative than those with phenyl phosphines. The electron-donating ability of the amine group also influences the reduction potentials, despite its distance from the Rh center. More basic amine groups contribute to more negative reduction potentials, as can clearly be seen when the phenyl phosphine substituent is kept constant. In the case of phenylphosphine containing ligands, the reduction potentials span a range of 0.2 V as the amine substituent changes.

Thermodynamic Measurements. *Reactivity of $[Rh(P_2N_2)_2]BF_4$ Complexes with H_2 in the Absence of a Base.*

DOI: 10.1021/jacs.5b04291
J. Am. Chem. Soc. 2015, 137, 8251−8260

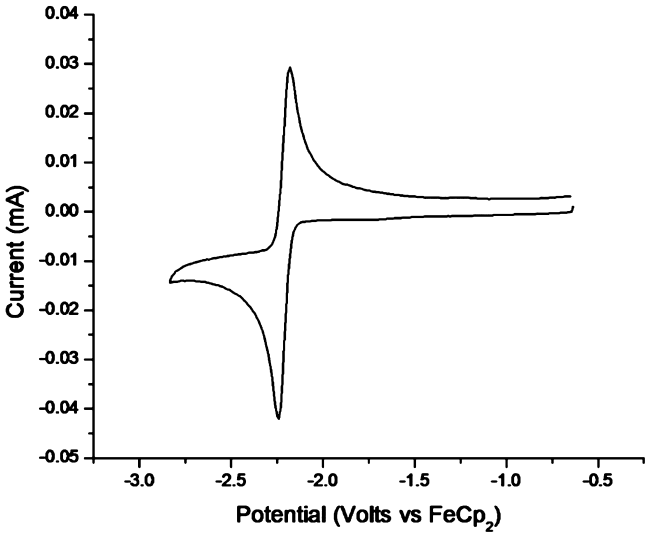

Figure 4. Cyclic voltammogram of 1 mM $[Rh(P^{Ph}{}_2N^{Ph}{}_2)_2](BF_4)$ (**1**) showing a typical voltammogram of $[Rh(P_2N_2)_2]^+$ complexes. Conditions: 0.2 M NBu_4PF_6 in acetonitrile, glassy carbon working and counter electrodes, 100 mV/s scan rate.

Rhodium diphosphine complexes are known to react with H_2 in the absence of a base to form six-coordinate dihydride complexes.[13,25] In order to investigate the effect of the pendant base on this process, we reacted complexes **1**−**5** with 1 atm of H_2 in THF-d_8 and studied the products by $^{31}P\{^1H\}$ NMR. All five complexes incompletely reacted to form what is assigned as the dihydride product, based on the appearance of two apparent doublets of triplets in the $^{31}P\{^1H\}$ NMR (Table S1). For the phenyl phosphine complexes, there is a large separation between the two ^{31}P peaks, indicating the two phosphorus environments are very different; these complexes are tentatively assigned to be *cis* dihydrides. For the cyclohexyl phosphine complexes, the two triplets are very close to each other indicating there are two similar phosphorus environments, and these complexes are tentatively assigned to be *trans* dihydrides. In this case, the added steric bulk of the cyclohexyl substituents likely disfavors the *cis* dihydride configuration. The equilibrium constants for the reaction of the $[Rh(P_2N_2)_2]^+$ complexes with H_2 were measured ($K_{H2} = [H_2Rh^+]/[Rh^+][H_2]$, where the concentration of H_2 is expressed in atmospheres) by the integration of the ^{31}P NMR spectra at 21 °C (Table 4). The dihydride resonances could not be resolved in the ^1H NMR, and likely overlap other resonances, but no peaks corresponding to a protonated amine were observed and no phosphorus peaks corresponding to the $HRh(P_2N_2)_2$ complexes were seen in the ^{31}P NMR, indicating that the pendant amine arms are not acting as unassisted bases. In all cases, when an excess of Verkade's base is present, the dihydride species were deprotonated and an equilibrium between the monohydride and Rh^+ complexes was established (shown by the hydricity equilibration experiments discussed below).

Hydricities of and Acidities of the $HRh(P_2N_2)_2$ Complexes. The reaction of $[Rh(P^{Ph}{}_2N^{Bn}{}_2)_2]BF_4$ (**2**), $[Rh(P^{Ph}{}_2N^{PhOMe}{}_2)_2]BF_4$ (**3**), $[Rh(P^{Cy}{}_2N^{Ph}{}_2)_2]BF_4$ (**4**), and $[Rh(P^{Cy}{}_2N^{PhOMe}{}_2)_2]BF_4$ (**5**) with H_2 in the presence of Verkade's base (2,8,9-triisopropyl-2,5,8,9-tetraaza-1-phosphabicyclo[3,3,3]undecane) resulted in two simultaneous equilibria between the $[Rh(P_2N_2)_2]^+$ and $HRh(P_2N_2)_2$ species and the protonated and deprotonated base, as shown in eq 1. If the solutions are purged with N_2 after reaching equilibrium, the spectra revert to those of the starting complex and the deprotonated base, confirming the reversibility of this activation. Verkade's base (pK_a of 33.63 in acetonitrile)[26] was convenient because it is a weakly nucleophilic phosphorus-containing base with ^{31}P signals that do not overlap with those of the HRh and Rh^+ complexes, allowing for the determination of the relative equilibrium ratios of the Rh complexes and the base and conjugate acid by integration of the ^{31}P resonances. Benzonitrile was used for solubility reasons (equilibrium values obtained in benzonitrile are expected to be a good estimate for equilibrium values in acetonitrile, which is the solvent most commonly used for these measurements).[15]

Using the thermodynamic cycle shown in Scheme 1, the free energies associated with reactions 1−3 can be used in eq 4 to calculate the hydride donor abilities, $\Delta G^\circ{}_H{}^-$. Verkade's base proved to be too basic to establish an equilibrium in the reaction with complex **1** and H_2, which led to complete formation of the $HRh(P^{Ph}{}_2N^{Ph}{}_2)_2$ complex, so this hydricity was not measured. On the basis of the dominance of the hydride product, however, it is expected that this is the least hydridic complex in this report. With the thermodynamic cycle shown in Scheme 2, the free energies associated with reactions 5−7 can be used in eq 8 to calculate the pK_a's of the $HRh(P_2N_2)_2$ complexes.

The $HRh(P_2N_2)_2$ complexes have calculated hydricities that range from 28−32 kcal/mol, where a smaller $\Delta G^\circ{}_H{}^-$ indicates that the complex is a better hydride donor. These hydricities are comparable to those measured for other $HRh(disphosphine)_2{}^+$ complexes[15,25b,27] and are among the most hydridic values measured for $HM(disphosphine)_2$ complexes. On the basis of comparisons between previously reported hydricities for rhodium and nickel $HM(diphosphine)_2$ species (diphosphine = depe, dmpe),[24a,27] complexes **7**−**10** have a similar increase in hydricity of 24−28 kcal/mol compared with analogous $[HNi(P_2N_2)_2]^+$ complexes.[5a] The estimated pK_a's for the monohydride species range from 39−50, making these complexes some of the most basic of the $M(diphosphine)_2$ complexes. Their basicities are comparable to those measured for other Co and Rh diphosphine complexes.[15,17b,28]

Table 4. Thermodynamic and Electrochemical Data for $[Rh(P_2N_2)_2]BF_4$ Complexes

	complex	K_{H2} (atm^{-1})[a]	$\Delta G^\circ{}_{H2}$ (kcal/mol)	$E_{1/2}(Rh^{I/-I})$[b] (V vs $FeCp_2{}^{+/0}$)	K_{eq1}[c]	$\Delta G^\circ{}_H{}^-$ (kcal/mol)	pK_a of HRh
1	$[Rh(P^{Ph}{}_2N^{Ph}{}_2)_2]^+$	0.41	0.53	−2.21(0.03)	–	–	–
2	$[Rh(P^{Ph}{}_2N^{Bn}{}_2)_2]^+$	0.48	0.44	−2.43(0.02)	20.13(3.26)	28.1	44.8
3	$[Rh(P^{Ph}{}_2N^{PhOMe}{}_2)_2]^+$	0.30	0.72	−2.27(0.02)	0.15(0.03)	31.1	39.4
4	$[Rh(P^{Cy}{}_2N^{Ph}{}_2)_2]^+$	1.0	0	−2.39(0.03)	0.05(0.01)	31.7	46.0
5	$[Rh(P^{Cy}{}_2N^{PhOMe}{}_2)_2]^+$	0.67	0.42	−2.45(0.02)	0.91(0.19)	30.0	49.9
	$[Rh(depe)_2]^+$	0.25[d]	0.82[d]	–	–	28.1[d]	–

[a]Values measured in THF-d_8. [b]Values measured in acetonitrile [c]Values measured in benzonitrile. [d]Previously reported.[25a,27]

DOI: 10.1021/jacs.5b04291
J. Am. Chem. Soc. 2015, 137, 8251−8260

Scheme 1. Determination of Hydride Donor Abilities for $[Rh(P_2N_2)_2]^+$ Complexes

	$\Delta G°$ (kcal/mol)	
$HRh(P_2N_2)_2 + HB^+ \rightleftharpoons [Rh(P_2N_2)_2]^+ + B + H_2$	$-RT \ln K_{eq}$	(1)
$B + H^+ \rightleftharpoons HB^+$	$-1.364\ pK_a$	(2)
$H_2 \rightleftharpoons H^+ + H^-$	76.0	(3)
$HRh(P_2N_2)_2 \rightleftharpoons [Rh(P_2N_2)_2]^+ + H^-$	$\Delta G°_{H^-} = -RT \ln K_{eq} - 1.364\ pK_a + 76.0$	(4)

Scheme 2. Determination of pK_a of $HRh(P_2N_2)_2$ Complexes

	$\Delta G°$ (kcal/mol)	
$HRh(P_2N_2)_2 \rightleftharpoons [Rh(P_2N_2)_2]^+ + H^-$	$\Delta G°_{H^-}$	(5)
$[Rh(P_2N_2)_2]^+ + 2e^- \rightleftharpoons [Rh(P_2N_2)_2]^-$	$-nF[(E_{Rh(I/-I)}]$	(6)
$H^- \rightleftharpoons H^+ + 2e^-$	79.6 kcal/mol	(7)
$HRh(P_2N_2)_2 \rightleftharpoons [Rh(P_2N_2)_2]^- + H^+$	$\Delta G°_{H^+} = \Delta G°_{H^-} - nF[(E_{Rh(I/-I)}] - 79.6$ $pKa = \Delta G°_{H^+}/(2.303RT)$	(8)

Previous studies have shown that hydride donor abilities of d^8 $[HM(diphosphine)_2]^{n+}$ (M = Pd, Ni) are linearly correlated to the reduction potential of the d^8/d^9 couple, with complexes with more negative reduction potentials being better hydride donors (smaller $\Delta G°_{H^-}$ values). The d^9/d^{10} couple has been shown to be linearly correlated to the pK_a of the $[HM(diphosphine)_2]^{n+}$ complex.[14,18a,29] For the $[Rh(P_2N_2)_2]^+$ complexes in this report, the d^8/d^9 couple is significantly destabilized and the complexes show one redox couple corresponding to the d^8/d^{10} couple. The reduction potentials, which are influenced by the electron-donating ability of the ligands, should be correlated with both the hydricity and acidity of the corresponding Rh(I) hydride.

The linear correlation of the hydricity with the E^0 for the d^8/d^9 couple is robust for $[Ni(P_2N_2)_2]^{2+}$ complexes, indicating that there are no unusual thermodynamic consequences introduced by the incorporation of the pendant base into the ligand backbone in the case of nickel.[14] For the $[Rh(P_2N_2)_2]^+$ complexes in this study, the correlation between the reduction potential and the hydricity is slightly weaker. When the base is held constant, as in the complexes $[Rh(P^{Cy}_2N^{PhOMe}_2)_2]^+$ and $[Rh(P^{Ph}_2N^{PhOMe}_2)_2]^+$, the complex with the more negative reduction potential is more hydridic, consistent with trends previously seen. A disruption in this trend occurs when comparing the hydricities of $[Rh(P^{Ph}_2N^{Bn}_2)_2]^+$ to $[Rh(P^{Cy}_2N^{PhOMe}_2)_2]^+$ and $[Rh(P^{Ph}_2N^{PhOMe}_2)_2]^+$ to $[Rh(P^{Cy}_2N^{Ph}_2)_2]^+$. In both cases, even though the complex with the cyclohexyl phosphine has the more negative reduction potential, the phenyl phosphine complex with the more basic amine is more hydridic or has a similar hydricity. The pK_a of the pendant amine seems to have a significant effect on the hydricity of the $HRh(P_2N_2)_2$ complex, beyond any effect it has on the reduction potential of the Rh(I) complex.

Catalytic Hydrogenation of CO_2. Complexes **1**–**5** were active for CO_2 hydrogenation to formate at room temperature under two atmospheres of 1:1 CO_2/H_2 in the presence of Verkade's base (2,8,9-triisobutyl-2,5,8,9-tetraaza-1-phosphabicyclo[3.3.3]undecane). Catalytic studies were performed in a J. Young NMR tube, and the production of formate over 1 h was quantified by measuring the ^1H NMR signal for formate (8.7 ppm) relative to a benzene internal standard. The ^1H and ^{31}P NMR spectra were recorded every 3 to 5 min and the NMR tube was briefly placed in a vortex mixer between scans to allow for gas mixing. The turnover frequencies (TOF) for each complex (Table 5) were determined by the slope of the linear region of the plots of mM formate formed versus time (see Supporting Information). The turnover number (TON) was limited by the amount of base available to deprotonate the dihydride and stabilize formate, and the rates started to level off as the base was consumed. The CO_2 hydrogenation activity of a rhodium diphosphine complex without pendant amines, $[Rh(depe)_2]^+$, was also measured under the same conditions to see how its activity compared to $[Rh(P_2N_2)_2]^+$ complexes. $[Rh(depe)_2]^+$ was chosen because its $\Delta G°_{H^-}$ was previously measured to be 28.1 kcal/mol,[27] which is within the range of values for the $[Rh(P_2N_2)_2]^+$ complexes, so the electron density at the Rh center should be similar to the $[Rh(P_2N_2)_2]^+$ complexes; this comparison should allow better understanding of how the incorporation of the pendant amine influences catalytic rates beyond altering the electron density of the metal center. In the $^{31}P\{^1H\}$ NMR spectra obtained during catalysis for all complexes studied, only the starting material ($[Rh(diphosphine)_2]^+$) was observed. The lack of any observed dihydride or monohydride species suggests that H_2 addition is likely the slow step in catalysis.

Table 5. Rates of Hydrogenation of CO_2 for $[Rh(P_2N_2)_2]^+$ and $[Rh(depe)_2]^+$ in THF[a]

	complex[b]	$[M^+]$ (mM)	[base] (mM)	TOF (h^{-1})	TON[c]
1	$[Rh(P^{Ph}_2N^{Ph}_2)_2]^+$	0.98	494	590 ± 20	365
2	$[Rh(P^{Ph}_2N^{PhOMe}_2)_2]^+$	1.0	498	460 ± 70	325
3	$[Rh(P^{Ph}_2N^{Bn}_2)_2]^+$	0.92	520	240 ± 30	220
4	$[Rh(P^{Cy}_2N^{Ph}_2)_2]^+$	1.1	500	720 ± 60	406
5	$[Rh(P^{Cy}_2N^{PhOMe}_2)_2]^+$	0.90	494	630 ± 40	325
	$[Rh(depe)_2]^+$	1.0	520	1070 ± 60	515

[a]Conditions: 400 μL d_8THF-d_8, 1:1 CO_2/H_2, 2 atm at 21°. [b]BF_4 salts were used for all complexes. [c]TON in this case is the turnovers after running the reaction for 1 h.

Effects of Pendant Amines on Catalysis. The typical proposed mechanism for CO_2 hydrogenation by rhodium bis-diphosphine complexes includes the following steps: (1) H_2 addition to the Rh(I) cation to make the dihydride complex, (2) deprotonation of the dihydride to make the HRh(I) complex, and (3) hydride transfer to CO_2/formate loss.[11c,13,30] Incorporation of P_2N_2 ligands into catalysts for this process

DOI: 10.1021/jacs.5b04291
J. Am. Chem. Soc. 2015, 137, 8251–8260

could potentially affect any of the above steps via increased electron density at the metal center as well as the action of the pendant base during both hydrogen activation and deprotonation of the dihydride.

Increasing the electron-donating ability of the diphosphine ligand could lead to changes in the rates for CO_2 hydrogenation by destabilizing the monohydride species that reacts with CO_2. However, during catalysis no monohydride species were observed on the NMR time scale, indicating that the hydricity of the monohydride species is not the most prominent factor controlling the relative rates for CO_2 hydrogenation. This is further highlighted by the difference in rates of CO_2 hydrogenation by $[Rh(P^{Ph}_2N^{Bn}_2)_2]^+$ and $[Rh(depe)_2]^+$. These complexes have similar hydricities, but $[Rh(P^{Ph}_2N^{Bn}_2)_2]^+$ is a much slower catalyst than $[Rh(depe)_2]^+$.

Increasing the electron-donating ability of the ligands could also lead to changes in the rates by making the oxidative addition of H_2 more favorable; it has previously been shown that the increased electron-donating ability of the ligands makes the oxidative addition of H_2 more favorable in $[Rh(diphosphine)_2]^+$ complexes.[25a] The NMR time scale observation of only starting Rh(I) cation during catalysis may indicate that H_2 addition is the slow step in catalysis, with all subsequent steps being comparatively facile. However, it is clear that the influence of the pendant base on the rate of this activation is not dominated by ligand donation, as rates of catalysis do not trend with the ΔG°_{H2}. Finally, the pendant amine itself could be affecting catalytic rates by influencing H_2 addition or aiding in the deprotonation of dihydride species. Given that no monohydride is seen upon H_2 activation by the Rh(I) complexes in the absence of an external base, we can rule out direct deprotonation of this species by the pendant base. Instead, the base may act thermodynamically by destabilizing the product of H_2 addition or kinetically by facilitating deprotonation by Verkade's base.

The lack of a strong correlation between the ΔG°_{H2} values in the absence of an external base and the catalytic rates and the fact that H_2 addition seems to be the rate-determining step in catalysis may indicate that the dominant factor in catalysis is the ability of the external base to come close enough to the metal center to assist in the oxidative addition of H_2. $[Rh(depe)_2]^+$, which is the least sterically hindered, shows the fastest rate, with all of the P_2N_2 complexes being significantly slower. The rates also seem to trend with the increased bulk of the pendant amine more generally, decreasing as the amine becomes bulkier. In effect, because the pendant base cannot directly deprotonate the dihydride species, its presence can only improve catalysis by increasing the electron density at the metal center. However, because initial activation of H_2 by the combined action of the Rh(I) center and the external base appears to be the rate-determining step, the added steric bulk of the P_2N_2 ligand outweighs any benefit conferred by increasing the donation of the ligand. A conclusive study on this matter would ideally use an equally strong, less sterically hindered external base, but it is difficult to find a base in this pK_a range that is smaller and non-nucleophilic. When catalysis was attempted with a weaker base, triethylamine, no formate production was observed under the conditions used.

The lack of any benefit to catalysis due to the addition of the pendant base highlights the importance of assuring that no steps in a catalytic cycle are substantially mismatched in energy. We initially hoped that the addition of the pendant amine would help to increase the rates for H_2 splitting, and that by using a strongly basic metal, we would see increased rates in CO_2 hydrogenation. However, while the use of such a strong hydride forming metal with very donating ligands produced an extremely strong Rh(I) hydride donor for CO_2 hydrogenation, it also produced a strongly basic dihydride precursor that could not be deprotonated by the pendant amine, negating any benefit from having the pendant base in the second coordination sphere. As noted by others, the best catalysts of this type would have a monohydride strong enough to activate CO_2, but such an intermediate would not be so basic that the dihydride species could not be easily deprotonated.[30]

CONCLUSIONS

In this work, we introduce pendant amines in the form of 1,5-diaza-3,7-diphosphacyclooctane P_2N_2 ligands to the $[Rh(disphosphine)_2]^+$ platform, extending the rich chemistry of these proton-relay-containing ligands to rhodium. Along with the synthesis and characterization of the $[Rh(P_2N_2)_2]^+$ complexes, we were able to synthesize and characterize the corresponding $HRh(P_2N_2)_2$ complexes, as well as obtain structural data for the $HRh(P^{Ph}_2N^{Bn}_2)_2$, $HRh(P^{Ph}_2N^{PhOMe}_2)_2$ and $HRh(P^{Cy}_2N^{Ph}_2)_2$ complexes. These structures represent only the second examples of X-ray structures of $[HM(P_2N_2)_2]^{n+}$ complexes, and the first where the hydride ligands could be resolved explicitly in the difference maps. These structures show possible hydrogen bonding interactions between the pendant amine and the hydride ligands, as has previously been proposed based on structural, NMR, and computational studies for $[HNi(P_2N_2)]^+$ complexes.

We also studied the possibility of enhancing CO_2 reduction activity of the rhodium diphosphine platform through the addition of functionality into the second coordination sphere, as has been fruitfully explored in the design of hydrogenase mimics, but is only starting to be investigated in CO_2 hydrogenation catalysis.[12,13] To gain a better understanding of how the series of pendant amine containing disphosphine ligands affect catalytic activity, we measured the hydricities of several of the complexes, estimated their pK_a's, measured their relative affinities for H_2 addition, and measured their rates for CO_2 hydrogenation.

The P_2N_2 complexes in this study are catalytically active for CO_2 hydrogenation, but their CO_2 hydrogenation activity was lower than a nonpendant-amine-containing Rh diphosphine complex with a hydricity in the same range as the P_2N_2 complexes. The data suggest that the added steric bulk of the P_2N_2 ligands hinders catalysis despite the strong reducing power of the relevant monohydride intermediates.

EXPERIMENTAL METHODS

Unless otherwise noted, all reactions were carried out under a N_2 atmosphere using standard Schlenk and glovebox techniques. Acetone was dried over 4 Å molecular sieves and degassed prior to use. All other solvents used were dried over activated molecular sieves and alumina and degassed prior to use. The diphosphine ligands $P^{Ph}_2N^{Ph}_2$, $P^{Cy}_2N^{Ph}_2$, $P^{Ph}_2N^{PhOMe}_2$, $P^{Cy}_2N^{PhOMe}_2$, and $P^{Ph}_2N^{Bn}_2$ were synthesized as previously reported.[5a,14] All other chemicals were obtained from commercial suppliers and used without further purification. ^1H and $^{31}P\{^1H\}$ NMR spectra were recorded using a 300 or 500 MHz Varian spectrometers. ^1H NMR chemical shifts were referenced against the residual solvent signal and are reported in ppm downfield of tetramethylsilane (δ = 0). $^{31}P\{^1H\}$ NMR chemical shifts were externally referenced to phosphoric acid (85%). Mass spectrometry data was collected on a Finnagan LCQDECA in ESI positive ion

DOI: 10.1021/jacs.5b04291
J. Am. Chem. Soc. 2015, 137, 8251−8260

mode. Elemental analyses were performed by Midwest Microlabs, LLC in Indianapolis, Indiana.

Syntheses. *(1). [Rh($P^{Ph}_2N^{Ph}_2$)$_2$]BF_4.* In a 10 mL Schlenk flask, Chloro(1,5-cyclooctadiene)rhodium(I) dimer (0.228 g, 0.462 mmol) and silver tetrafluoroborate (0.180 g, 0.925 mmol) were slurried in 5 mL acetone. The mixture was allowed to stir for 1 h. In a 100 mL Schlenk flask, $P^{Ph}_2N^{Ph}_2$ (0.834 g, 1.85 mmol) was dissolved in 50 mL of methylene chloride. The AgCl that precipitated out in the first flask was filtered out and the yellow filtrate was added to the 100 mL flask containing the ligand, producing an orange solution. The solution was allowed to stir overnight. The solution was reduced and diethyl ether was added, forming a yellow precipitate. The precipitate was collected to obtain 0.783 g (61%) of a yellow powder. ^{1}H NMR (500 MHz, CD_3CN) δ 7.46−7.40 (m, 8H, Ar*H*), 7.30−7.14 (m, 12H, Ar*H*), 7.10 (t, J = 7.6 Hz, 8H, Ar*H*), 7.04−6.88 (m, 12H, Ar*H*), 4.05 (s, 16H, PCH_2N). ^{31}P{^{1}H} NMR (121 MHz, CD_3CN) δ 5.38 (d, J_{Rh-P} = 123.7 Hz). HRMS (ESI-TOF) m/z [M − BF_4]$^+$ Calc. for $C_{56}H_{56}N_4P_4Rh$ 1011.2505, found 1011.2501, 100%. Elemental Anal. Calc. for $C_{56}H_{56}N_4P_4Rh$: C, 61.22%; H, 5.14%; N, 5.10%. Found: C, 61.28%; H, 5.10%; N, 5.06%.

(2). [Rh($P^{Ph}_2N^{Bn}_2$)$_2$]BF_4. This complex was synthesized using a procedure similar to that for [Rh($P^{Ph}_2N^{Ph}_2$)$_2$]BF_4 in 70% yield. ^{1}H NMR (500 MHz, CD_3CN) δ 7.50−7.24 (m, 20H, Ar*H*), 7.12−7.06 (m, 4H, Ar*H*), 6.97−6.84 (m, 16H, Ar*H*), 4.30 (s, 8H, CH_2 benzyl), 3.62 (d, J = 13.1 Hz, 8H, PCH_2N), 3.31 (d, J = 13.1 Hz, 8H, PCH_2N). ^{31}P{^{1}H} NMR (121 MHz, CD_3CN) δ −2.71 (d, J_{Rh-P} = 120.3 Hz). HRMS (ESI-TOF) m/z [M − BF_4]$^+$ Calc. for $C_{60}H_{64}N_4P_4Rh$ 1067.3131, found 1067.3128, 100%. Elemental Anal. Calc. for $C_{60}H_{64}BF_4N_4P_4Rh$: C, 62.41%, H, 5.59%; N, 4.85%. Found: C, 62.21%; H, 5.56%; N, 4.97%.

(3). [Rh($P^{Ph}_2N^{PhOMe}_2$)$_2$]BF_4. This complex was synthesized using a procedure similar to that for [Rh($P^{Ph}_2N^{Ph}_2$)$_2$]BF_4 in 94% yield. ^{1}H NMR (500 MHz, CD_3CN) δ 7.29−7.21 (m, 8H, Ar*H*), 7.21−7.12 (m, 4H, Ar*H*), 7.10−6.98 (m, 16H, Ar*H*), 6.95−6.87 (m, 8H, Ar*H*), 3.97 (s, 16H, PCH_2N), 3.75 (s, 12H, OCH_3). ^{31}P{^{1}H} NMR (121 MHz, CD_3CN) δ 3.87 (d, J_{Rh-P} = 123.5 Hz). HRMS (ESI-TOF) m/z [M − BF_4]$^+$ Calc. for $C_{60}H_{64}N_4O_4P_4Rh$ 1131.2928, found 1131.2924, 100%. Elemental Anal. Calc. For $C_{60}H_{64}BF_4N_4O_4P_4Rh$: C, 59.13%; H, 5.29%; N, 4.60%. Found: C, 59.23%; H, 5.55%, N, 4.60%.

(4). [Rh($P^{Cy}_2N^{Ph}_2$)$_2$]BF_4. This complex was synthesized using a procedure similar to that for [Rh($P^{Ph}_2N^{Ph}_2$)$_2$]BF_4 in 82% yield. ^{1}H NMR (500 MHz, CD_3CN) δ 7.23−7.18 (m, 8H, Ar*H*), 7.08−7.03(m, 8H, Ar*H*), 6.88−6.83 (m, 4H), 3.80 (s, br, 16H, PCH_2N), 1.95−0.99 (m, 40H, CH_2 cyclohexyl). ^{31}P{^{1}H} NMR (121 MHz, CD_3CN) δ 9.6 (d, J_{Rh-P} = 122.4 Hz). HRMS (ESI-TOF) m/z [M − BF_4]$^+$ Calc. for $C_{56}H_{80}N_4P4Rh$ 1035.4383, found 1035.4381, 100%. Elemental Anal. Calc. for $C_{56}H_{80}BF_4N_4P_4Rh$: C, 59.90%; H, 7.18%; 4.99%. Found: C, 58.99%; H, 7.12%; N, 4.94%.

(5). [Rh($P^{Cy}_2N^{PhOMe}_2$)$_2$]BF_4. This complex was synthesized using a procedure similar to that for [Rh($P^{Ph}_2N^{Ph}_2$)$_2$]BF_4 in 59% yield. ^{1}H NMR (500 MHz, CD_3CN) δ 7.09 (d, J = 9.0 Hz, 8H, Ar*H*), 6.78 (d, J = 9.0 Hz, 8H, Ar*H*), 3.7−3.65 (m, 16H, PCH_2N) 3.67 (s, 12H, OCH_3), 1.97−0.70 (m, 40H, CH_2 cyclohexyl). ^{31}P{^{1}H} NMR (121 MHz, CD_3CN) δ 8.09 (d, J_{Rh-P} = 122.6 Hz). HRMS (ESI-TOF) m/z [M − BF_4]$^+$ Calc. for $C_{60}H_{88}N_4O_4P_4Rh$ 1155.4806, found 1155.4803, 100%. Elemental Anal. Calc. for $C_{60}H_{88}N_4O_4P_4Rh$: C, 57.98%; H, 7.14%; N, 4.51%. Found: C, 57.54%; H, 6.97%; N, 4.28%.

(6). HRh($P^{Ph}_2N^{Ph}_2$)$_2$. 0.113 g (0.103 mmol) of [Rh($P^{Ph}_2N^{Ph}_2$)$_2$]BF_4 was added to a vial with a stir bar along with 10 mL of toluene. 124 μL of a solution of 1 M $NaHBEt_3$ in toluene (0.125 mmol) was added to the stirring solution via syringe. The yellow solution began to turn orange and formed an orange precipitate. The solution was stirred overnight and the toluene was then removed. The orange product was dissolved in 10 mL of THF and filtered to remove the $NaBF_4$. The THF solution was layered with 10 mL of pentane and cooled to −35 °C. The next day the orange precipitate was collected and dried in a vacuum to yield 0.058 g product (56%). ^{1}H NMR (500 MHz, C_6D_6) δ 7.55 (broad s, 8H, Ar*H*), 7.14−7.05 (m, 8H, Ar*H*), 7.04−6.94 (m, 12H, Ar*H*), 6.88−6.73 (m, 12H, Ar*H*), 3.91 (d, J = 13.0 Hz, 8H, PCH_2N), 3.57 (d, J = 13.0 Hz, 8H, PCH_2N), −8.43 (pd, J = 27.3, 14.5 Hz, 1H, Rh*H*). ^{31}P{^{1}H} NMR (121 MHz, C_6D_6) δ 16.06 (d, J_{Rh-P} = 129.2 Hz). ESI-MS (m/z) 1012.3, [M]$^+$, 63%, 1011.3, [M − H]$^+$, 100%. Elemental Anal. Calc. for $C_{56}H_{57}N_4P_4Rh$: C, 66.40%; H, 5.67%; N, 5.53%. Found: C, 66.17%; H, 5.58%; N, 5.51%.

(7). HRh($P^{Ph}_2N^{Bn}_2$)$_2$. Complex was synthesized using a procedure similar to that for HRh($P^{Ph}_2N^{Ph}_2$)$_2$ in 50% yield. ^{1}H NMR (500 MHz, C_6D_6) δ 7.95−7.50 (m, 8H, Ar*H*), 7.28−7.19 (m, 8H, Ar*H*), 7.18−6.91 (m, 24H, Ar*H*), 3.67 (s, 8H, CH_2 benzyl), 3.33 (d, J = 11.8 Hz, 8H, PCH_2N), 2.78 (d, J = 11.8 Hz, 8H, PCH_2N), −7.66 (pd, J = 26.2, 17.6 Hz, 1H, Rh*H*). ^{31}P{^{1}H} NMR (121 MHz, C_6D_6) δ 9.05 (d, J_{Rh-P} = 129.4 Hz). ESI-MS (m/z) 10168.3, [M]$^+$, 66%, 1067.3, [M − H]$^+$, 100%. Elemental Anal. Calc. for $C_{60}H_{65}N_4P_4Rh$: C, 67.41%, H, 6.13%; N, 5.42%. Found: C, 67.33%; H, 6.20%; N, 5.20%.

(8). HRh($P^{Ph}_2N^{PhOMe}_2$)$_2$. This complex was synthesized using a procedure similar to that for HRh($P^{Ph}_2N^{Ph}_2$)$_2$ in 75% yield. ^{1}H NMR (500 MHz, C_6D_6) δ 7.61 (broad s, 8H, Ar*H*), 7.07−7.00 (m, 12H, Ar*H*), 6.91−6.83 (m, 8H, Ar*H*), 6.83−6.72 (m, 8H, Ar*H*), 3.94 (d, J = 12.7 Hz, 8H, PCH_2N), 3.59 (d, J = 12.7 Hz, 8H, PCH_2N), 3.36 (s, 12H, CH_3O), −8.32 (pd, J = 26.8, 14.1 Hz, 1H, Rh*H*). ^{31}P{^{1}H} NMR (121 MHz, C_6D_6) δ 13.79 (d, J_{Rh-P}= 128.6 Hz). ESI-MS (m/z) 1132.2, [M]$^+$, 57%, 1131.2, [M − H]$^+$, 100%. Elemental Anal. Calc. for $C_{60}H_{65}N_4P_4Rh$: C, 63.61%; H, 5.78%, 4.95%. Found: C, 62.80%; H, 5.81%; N, 5.00%.

(9). HRh($P^{Cy}_2N^{Ph}_2$)$_2$. This complex was synthesized using a procedure similar to that for HRh($P^{Ph}_2N^{Ph}_2$)$_2$ in 60% yield. ^{1}H NMR (500 MHz, C_6D_6) δ 7.27−7.21 (m, 8H, Ar*H*), 7.10−7.04 (m, 8H, Ar*H*), 6.88−6.82 (m, 4H, Ar*H*), 3.44 (q, J = 12.5 Hz, 16H, PCH_2N), 1.77−0.69 (m, 40H, CH_2 cyclohexyl), −10.27 (pd, J = 23.5, 12.1 Hz, 1H). ^{31}P{^{1}H} NMR (121 MHz, C_6D_6) δ 21.72 (d, J_{Rh-P} = 128.2 Hz). ESI-MS (m/z) 1036.4, [M]$^+$, 63%, 1035.4, [M − H]$^+$, 100%. Elemental Anal. Calc. for $C_{60}H_{81}N_4P_4Rh$: C, 64.86%; H, 7.87%; N, 5.40%. Found: C, 64.21%; H, 7.72%; N, 5.45%.

(10). HRh($P^{Cy}_2N^{PhOMe}_2$)$_2$. This complex was synthesized using a procedure similar to that for HRh($P^{Ph}_2N^{Ph}_2$)$_2$ in 72% yield. ^{1}H NMR (500 MHz, C_6D_6) δ 7.10−7.03 (m, 8H, Ar*H*), 6.92−6.80 (m, 8H, Ar*H*), 3.45 (d, J = 12.2 Hz, 8H, PCH_2N), 3.42−3.35 (s (OCH_3, 12H) overlaid by d (PCH_2N, 8H), 1.94−0.73 (m, 40H, CH_2 cyclohexyl), −10.20 (dp, J = 23.3, 12.1 Hz, 1H). ^{31}P{^{1}H} NMR (121 MHz, C_6D_6) δ 21.67 (d, J_{Rh-P} = 131.5 Hz). ESI-MS (m/z) 1156.4, [M]$^+$, 59%, 1055.4, [M − H]$^+$, Elemental Anal. Calc. for $C_{60}H_{89}N_4O_4P_4Rh$: C, 62.28%; H, 7.75%, N, 4.48%. Found: C, 62.21%; H, 7.80%; N, 4.48%.

Electrochemical Studies. Electrochemical experiments were performed using a BAS Epsilon potentiostat. Cyclic voltammograms (CV's) were performed under nitrogen in a one compartment cell using a glassy carbon BASi working electrode, a glassy carbon rod counter electrode, and a nonaqueous Ag reference electrode from BASi that contained an acetonitrile solution of 0.2 M NBu_4PF_6 and 1 mM $AgNO_3$. All experiments were performed in dry acetonitrile using 0.2 M NBu_4PF_6 as the supporting electrolyte. After taking initial CV's, Cp_2Co^+ was added as in internal reference. Then, a clean electrolyte solution was made and another CV of Cp_2Co^+ was taken to confirm that the reference electrode was stable. The position of the Cp_2Co^+ couple was then used to reference the reduction potentials of the complexes to the Cp_2Fe^+/Cp_2Fe couple.

Crystallography. Crystals of the Rh complexes suitable for X-ray structural determinations were mounted in polybutene oil on a glass fiber and transferred on the goniometer head to the precooled instrument (100 K). Data was collected on either a Bruker P4, Platform, D8 Venture, or Kappa Apex II diffractometer. Crystallographic measurements were carried out using Mo Kα radiation (λ = 0.71073 Å) or Cu Ka radiation (λ = 1.54178 Å) All structures were solved by direct methods using OLEX2 and refined with full-matrix least-squares procedures using SHELXL-97. All non-hydrogen atoms were anisotropically refined unless otherwise reported. The hydrogen atoms were included in calculated positions as riding models in the refinement, unless otherwise reported.

General Procedure for Hydricity Determination by Heterolytic H_2 Cleavage. [Rh($P^{Ph}_2N^{PhOMe}_2$)$_2$]BF_4. In a typical experiment, [Rh($P^{Ph}_2N^{PhOMe}_2$)$_2$]BF_4 (10−16 mg, 0.009−0.013 mmol) and 2,8,9-triisopropyl-2,5,8,9-tetraaza-1-phosphabicyclo[3,3,3]undecane (7.5−

DOI: 10.1021/jacs.5b04291
J. Am. Chem. Soc. 2015, 137, 8251−8260

16 mg, 0.02−0.04 mg) were weighed into 3 J. Young NMR tubes and dissolved in 0.5 mL of benzonitrile. The tubes were evacuated and an atmosphere of H_2 was introduced. After 2 weeks an equilibrium was reached indicated by a constant ratio of products. Integration of each of the peaks of the 4 species in the ^{31}P NMR spectra allowed for the determination of the relative ratios and these were used to determine the equilibrium constant. Equilibrium constants were calculated using the average of data obtained from 3 experiments.

General Procedure for the Reaction of H_2 Gas with $[Rh(P_2N_2)_2]$-BF_4 Complexes. An NMR tube capped with a rubber septa containing 0.043 M THF-d_8 was purged with H_2 for 10 min using a needle. ^{31}P NMR spectra were recorded and integrated to determine the relative ratios of $[Rh(P_2N_2)_2]^+$ to $[H_2Rh(P_2N_2)_2]^+$ complexes. Equilibrium constants were calculated using the average of data obtained from 3 experiments.

General Procedure for Catalysis. In a glovebox, ∼400 mg of Verkade's base (2,8,9-triisobutyl-2,5,8,9-tetraaza-1-phosphabicyclo-[3.3.3]undecane) was dissolved in 2 mL of THF-d_8 to make the base concentration ∼500 mM. The appropriate amount of catalysts was added to make catalysts concentration ∼1 mM. 4 μL of benzene was added as an internal standard for the quantification of formate. 400 μL of this solution was added to 3 J. Young NMR tubes. The tubes were freeze−pump−thawed to remove N_2 and then backfilled with 1 atm of CO_2. They were then frozen with liquid N_2 just up to the solvent line to condense the CO_2 and then an atmosphere of H_2 was introduced to the headspace to make the overall pressure ∼2 atm of 1:1 CO_2/H_2. The tube was brought to room temperature and briefly placed in a vortex mixer to allow for gas mixing and quantitative ^1H NMR and $^{31}P\{^1H\}$ were collected between 2 to 5 min apart for 1 h. Between scans the tube was placed in a vortex mixer briefly to allow for gas mixing. The amount of conversion at each point was measured by comparing the integral of the benzene peak with the formate peak. Turnover frequencies were calculated from the slope of the linear portions of the plots of time versus the amount of formate. The turnover frequencies given are an average for three experiments.

■ ASSOCIATED CONTENT

Supporting Information

Crystallographic data, .cif files, supporting electrochemical data, supporting NMR spectra, and plots of formate formed over time. The Supporting Information is available free of charge on the ACS Publications website at DOI: 10.1021/jacs.5b04291.

■ AUTHOR INFORMATION

Corresponding Author

*ckubiak@ucsd.edu

Notes

The authors declare no competing financial interest.

■ ACKNOWLEDGMENTS

The authors would like to acknowledge the Air Force Office of Scientific Research through the MURI program for funding under AFOSR Award No. FA9550-101-0572 and the Joint Center of Artificial Photosynthesis, a DOE Energy Innovation Hub, for funding under the Award DE-SC0004993.

■ REFERENCES

(1) Tard, C.; Pickett, C. J. *Chem. Rev.* **2009**, *109*, 2245−2274.
(2) (a) G. Märkl, V.; Jin, G. Y.; Schoerner, C. *Tetrahedron Lett.* **1980**, *21*, 1409−1412. (b) Doud, M. D.; Grice, K. A.; Lilio, A. M.; Seu, C. S.; Kubiak, C. P. *Organometallics* **2012**, *31*, 779−782.
(3) (a) Wilson, A. D.; Newell, R. H.; McNevin, M. J.; Muckerman, J. T.; Rakowski DuBois, M.; DuBois, D. L. *J. Am. Chem. Soc.* **2006**, *128*, 358−366. (b) Wiese, S.; Kilgore, U. J.; DuBois, D. L.; Bullock, R. M. *ACS Catal.* **2012**, *2*, 720−727.
(4) Yang, J. Y.; Bullock, R. M.; Dougherty, W. G.; Kassel, W. S.; Twamley, B.; DuBois, D. L.; Rakowski DuBois, M. *Dalton Trans.* **2010**, *39*, 3001−3010.
(5) (a) Galan, B. R.; Schöffel, J.; Linehan, J. C.; Seu, C.; Appel, A. M.; Roberts, J. A. S.; Helm, M. L.; Kilgore, U. J.; Yang, J. Y.; DuBois, D. L.; Kubiak, C. P. *J. Am. Chem. Soc.* **2011**, *133*, 12767−12779. (b) Seu, C. S.; Appel, A. M.; Doud, M. D.; DuBois, D. L.; Kubiak, C. P. *Energy Environ. Sci.* **2012**, *5*, 6480−6490.
(6) (a) Rakowski DuBois, M.; DuBois, D. L. *Chem. Soc. Rev.* **2009**, *38*, 62−72. (b) Yang, J. Y.; Bullock, R. M.; Shaw, W. J.; Twamley, B.; Fraze, K.; DuBois, M. R.; DuBois, D. L. *J. Am. Chem. Soc.* **2009**, *131*, 5935−5945.
(7) (a) Rossen, K. *Angew. Chem., Int. Ed.* **2001**, *40*, 4611−4613. (b) Schrock, R. R.; Osborn, J. A. *J. Am. Chem. Soc.* **1976**, *98*, 2134−2143.
(8) (a) Evans, D. A.; Fu, G. C.; Hoveyda, A. H. *J. Am. Chem. Soc.* **1988**, *110*, 6917−6918. (b) Osborn, J. A.; Jardine, F. H.; Young, J. F.; Wilkinson, G. *J. Chem. Soc. A* **1966**, 1711−1732.
(9) (a) Huang, Y.; Sachtler, W. M. H. *J. Catal.* **1999**, *188*, 215−225. (b) Yoshida, T.; Okano, T.; Otsuka, S. *J. Chem. Soc., Chem. Commun.* **1979**, 870−871. (c) Galan, A.; De Mendoza, J.; Prados, P.; Rojo, J.; Echavarren, A. M. *J. Org. Chem.* **1991**, *56*, 452−454.
(10) Kuwano, R.; Sato, K.; Kurokawa, T.; Karube, D.; Ito, Y. *J. Am. Chem. Soc.* **2000**, *122*, 7614−7615.
(11) (a) Jessop, P. G.; Joó, F.; Tai, C.-C. *Coord. Chem. Rev.* **2004**, *248*, 2425−2442. (b) Leitner, W. *Angew. Chem., Int. Ed. Engl.* **1995**, *34*, 2207−2221. (c) Burgemeister, T.; Kastner, F.; Leitner, W. *Angew. Chem., Int. Ed. Engl.* **1993**, *32*, 739−741.
(12) (a) Schmeier, T. J.; Dobereiner, G. E.; Crabtree, R. H.; Hazari, N. *J. Am. Chem. Soc.* **2011**, *133*, 9274−9277. (b) Wang, W.-H.; Hull, J. F.; Muckerman, J. T.; Fujita, E.; Himeda, Y. *Energy Environ. Sci.* **2012**, *5*, 7923−7926. (c) Fujita, E.; Muckerman, J. T.; Himeda, Y. *Biochim. Biophys. Acta* **2013**, *1827*, 1031−1038.
(13) Bays, J. T.; Priyadarshani, N.; Jeletic, M. S.; Hulley, E. B.; Miller, D. L.; Linehan, J. C.; Shaw, W. J. *ACS Catal.* **2014**, *4*, 3663−3670.
(14) Fraze, K.; Wilson, A. D.; Appel, A. M.; Rakowski DuBois, M.; DuBois, D. L. *Organometallics* **2007**, *26*, 3918−3924.
(15) Price, A. J.; Ciancanelli, R.; Noll, B. C.; Curtis, C. J.; DuBois, D. L.; DuBois, M. R. *Organometallics* **2002**, *21*, 4833−4839.
(16) Garrou, P. E. *Chem. Rev.* **1981**, *81*, 229−266.
(17) (a) Aresta, M.; Dibenedetto, A.; Amodio, E.; Pápai, I.; Schubert, G. *Inorg. Chem.* **2002**, *41*, 6550−6552. (b) Ciancanelli, R.; Noll, B. C.; DuBois, D. L.; DuBois, M. R. *J. Am. Chem. Soc.* **2002**, *124*, 2984−2992. (c) Miedaner, A.; DuBois, D. L.; Curtis, C. J.; Haltiwanger, R. C. *Organometallics* **1993**, *12*, 299−303.
(18) (a) Wander, S. A.; Miedaner, A.; Noll, B. C.; Barkley, R. M.; DuBois, D. L. *Organometallics* **1996**, *15*, 3360−3373. (b) Albright, T. A.; Hoffmann, R.; Thibeault, J. C.; Thorn, D. L. *J. Am. Chem. Soc.* **1979**, *101*, 3801−3812. (c) Elian, M.; Hoffmann, R. *Inorg. Chem.* **1975**, *14*, 1058−1076.
(19) (a) Pruchnik, F. P.; Smoleński, P.; Gałdecka, E.; Gałdecki, Z. *Inorg. Chem. Acta* **1999**, *293*, 110−114. (b) Ball, R. G.; James, B. R.; Mahajan, D.; Trotter, J. *Inorg. Chem.* **1981**, *20*, 254−261. (c) McLean, M. R.; Stevens, R. C.; Bau, R.; Koetzle, T. F. *Inorg. Chim. Acta* **1989**, *166*, 173−175.
(20) Das, P.; Stolley, R. M.; van der Eide, E. F.; Helm, M. L. *Inorg. Chem.* **2014**, *2014*, 4611−4618.
(21) O'Hagan, M.; Shaw, W. J.; Raugei, S.; Chen, S.; Yang, J. Y.; Kilgore, U. J.; DuBois, D. L.; Bullock, R. M. *J. Am. Chem. Soc.* **2011**, *133*, 14301−14312.
(22) Slater, S.; Wagenknecht, J. H. *J. Am. Chem. Soc.* **1984**, *106*, 5367−5368.
(23) Bard, A. J.; Faulkner, L. R. *Electrochemical Methods: Fundamentals and Applications*; John Wiley & Sons, Inc.: New York, 2000; p 856.
(24) (a) Berning, D. E.; Noll, B. C.; DuBois, D. L. *J. Am. Chem. Soc.* **1999**, *121*, 11432−11447. (b) Longato, B.; Riello, L.; Bandoli, G.; Pilloni, G. *Inorg. Chem.* **1999**, *38*, 2818−2823. (c) Berning, D. E.;

DOI: 10.1021/jacs.5b04291
J. Am. Chem. Soc. 2015, 137, 8251−8260

Miedaner, A.; Curtis, C. J.; Noll, B. C.; Rakowski DuBois, M. C.; DuBois, D. L. *Organometallics* **2001**, *20*, 1832−1839.
(25) (a) DuBois, D. L.; Blake, D. M.; Miedaner, A.; Curtis, C. J.; DuBois, M. R.; Franz, J. A.; Linehan, J. C. *Hydride Transfer from Rhodium Complexes to Triethylborane* **2006**, *25*, 4414−4419. (b) Raebiger, J. W.; DuBois, D. L. *Organometallics* **2004**, *24*, 110−118.
(26) Kisanga, P. B.; Verkade, J. G.; Schwesinger, R. *J. Org. Chem.* **2000**, *65*, 5431−5432.
(27) Mock, M. T.; Potter, R. G.; Camaioni, D. M.; Li, J.; Dougherty, W. G.; Kassel, W. S.; Twamley, B.; DuBois, D. L. *J. Chem. Soc., Chem. Commun.* **2009**, *131*, 14454−14465.
(28) Raebiger, J. W.; DuBois, D. L. *Organometallics* **2005**, *24*, 110−118.
(29) Raebiger, J. W.; Miedaner, A.; Curtis, C. J.; Miller, S. M.; Anderson, O. P.; DuBois, D. L. *J. Chem. Soc., Chem. Commun.* **2004**, *126*, 5502−5514.
(30) Jeletic, M. S.; Mock, M. T.; Appel, A. M.; Linehan, J. C. *J. Am. Chem. Soc.* **2013**, *135*, 11533−11536.

DOI: 10.1021/jacs.5b04291
J. Am. Chem. Soc. 2015, 137, 8251−8260